Does "Butyrylization" of Acetylcholinesterase through Substitution of the Six Divergent Aromatic Amino Acids in the Active Center Gorge Generate an Enzyme Mimic of Butyrylcholinesterase?†

Dana Kaplan,‡ Arie Ordentlich,‡ Dov Barak,§ Naomi Ariel,‡ Chanoch Kronman,‡ Baruch Velan,‡ and Avigdor Shafferman*,‡

Departments of Biochemistry & Molecular Genetics and Organic Chemistry, Israel Institute for Biological Research, Ness-Ziona 74100, Israel

Received January 29, 2001; Revised Manuscript Received March 28, 2001

ABSTRACT: The active center gorge of human acetylcholinesterase (HuAChE) is lined by 14 aromatic residues, whereas in the closely related human butyrylcholinesterase (HuBChE) 3 of the aromatic active center residues (Phe295, Phe297, Tyr337) as well as 3 of the residues at the gorge entrance (Tyr72, Tyr124, Trp286) are replaced by aliphatic amino acids. To investigate whether this structural variability can account for the reactivity differences between the two enzymes, gradual replacement of up to all of the 6 aromatic residues in HuAChE by the corresponding residues in HuBChE was carried out. The affinities of the hexamutant (Y72N/Y124Q/W286A/F295L/F297V/Y337A) toward tacrine, decamethonium, edrophonium, huperzine A, or BW284C51 differed by about 5-, 80-, 170-, 25000-, and 17000-fold, respectively, from those of the wild-type HuAChE. For most of these prototypical noncovalent active center and peripheral site ligands, the hexamutant HuAChE displayed a reactivity phenotype closely resembling that of HuBChE. These results support the accepted view that the active center architectures of AChE and BChE differ mainly by the presence of a larger void space in BChE. Nevertheless, reactivity of the hexamutant HuAChE toward the substrates acetylthiocholine and butyrylthiocholine, or covalent ligands such as phosphonates and the transition state analogue *m*-(*N*,*N*,*N*-trimethylammonio)trifluoroacetophenone (TMTFA), is about 45−170-fold lower than that of HuBChE. Most of this reduction in reactivity can be related to the combined replacements of the three aromatic residues at the active center, Phe295, Phe297, and Tyr337. We propose that the hexamutant HuAChE, unlike BChE, is impaired in its capacity to accommodate certain tetrahedral species in the active center. This impairment may be related to the enhanced mobility of the catalytic histidine His447, which is observed in molecular dynamics simulations of the hexamutant and the F295L/F297V/Y337A HuAChE enzymes but not in the wild-type HuAChE.

Acetylcholinesterase (AChE,[1] EC 3.1.1.7) is a serine hydrolase whose function at the cholinergic synapse is the rapid hydrolysis of the neurotransmitter acetylcholine (ACh). X-ray structures of AChEs from various sources (*Torpedo californica*, TcAChE; mouse, MoAChE; human, HuAChE; *Drosophila*, DAChE) show that the catalytic site is located near the bottom of a deep and narrow "gorge", which penetrates halfway into the enzyme (*1*−*4*). One of the striking features of this gorge is related to the presence of 14 aromatic residues, which line about 40% of its surface and which are highly conserved in enzymes from different species (*5*). This complex array of aromatic residues was hypothesized to provide a guidance mechanism facilitating a two-dimensional diffusion of ACh into the active site (*5*−*7*) as well as for substrate accommodation (*7*−*11*). Yet, butyrylcholinesterase (BChE, acylcholine acyl hydrolase, EC 3.1.1.8), another type of cholinesterase found in vertebrates, catalyzes ACh hydrolysis as efficiently as AChE, although six of the active site gorge aromatic residues (72, 124, 286, 295, 297, and 337, HuAChE numbering) are replaced by aliphatic amino acids (*12*, *13*). On the other hand, AChE and BChE exhibit distinct substrate and inhibitor selectivities (*14*, *15*), and some of the differences have been directly associated with the nature of the amino acids at each of these six positions (*8*−*10*, *16*, *17*).

Early hypotheses (*18*, *19*) and modeling experiments (*12*, *20*) indicated that the main functional difference between the AChE and BChE active sites is related to the structure

† This work was supported by the U.S. Army Research and Development Command, Contracts DAMD17-96-C-6088 and DAMD17-00-C-0021 (to A.S.).

* Corresponding author. Tel: (972)-8-9381595. Fax: (972)-8-9401404. E-mail: avigdor@iibr.gov.il.

‡ Department of Biochemistry & Molecular Genetics.

§ Department of Organic Chemistry.

[1] Abbreviations: AChE, acetylcholinesterase; ACh, acetylcholine; TcAChE, *Torpedo californica* acetylcholinesterase; MoAChE, mouse acetylcholinesterase; HuAChE, human acetylcholinesterase; DAChE, *Drosophila* acetylcholinesterase; BChE, acylcholine acyl hydrolase; BCh, butyrylcholine; DFP, diisopropyl phosphorofluoridate; paraoxon, *p*-nitrophenyl diethyl phosphate; tacrine, 9-amino-1,2,3,4-tetrahydroacridine hydrochloride hydrate; BW284C51, di(*p*-allyl-*N*-dimethylaminophenyl)pentan-3-one; BTC, butyrylthiocholine; ATC, acetylthiocholine, edrophonium, ethyl(*m*-hydroxyphenyl)dimethylammonium chloride; decamethonium, 1,10-bis(trimethylammonium)decane; TMTFA, *m*-(*N*,*N*,*N*-trimethylammonio)trifluoroacetophenone; IBMPF, 2-butyl methylphosphonofluoridate; soman, 1,2,2-trimethylpropyl methylphosphonofluoridate; ChE, cholinesterase; iso-OMPA, tetraisopropylpyrophosphoramide; DEFP, diethyl phosphorofluoridate; VX, *O*-ethyl-*S*-[2-[bis(1-methylethyl)amino]ethyl] methylphosphonothioate.

10.1021/bi010181x CCC: $20.00
Published on Web 05/26/2001

of the acyl pocket, where residues corresponding to Phe295-(288)[2] and Phe297(290) are replaced by Leu and Val, respectively. Indeed, studies of AChE by site-directed mutagenesis and enzyme kinetics indicated that the acyl pocket residue Phe295 and to a lesser extent Phe297 determine specificity for phosphylating agents (*21*, *22*) and for the acyl moiety of substrates (*8*, *9*, *12*, *17*), mainly by limiting the pocket size. Accordingly, BChE is more reactive than AChE toward bulky substrates such as butyrylcholine (BCh) or organophosphorus inhibitors such as diisopropyl phosphofluoridate (DFP) or paraoxon. In a similar manner, the about 5-fold higher affinity of BChE toward the active center inhibitor tacrine, as compared to that of AChE, can be related to the absence of an aromatic residue in position 337 (Tyr in HuAChE and Ala in BChE) (*17*, *23*, *24*).

These results as well as similar mutagenesis studies conducted on BChE (*25*, *26*) suggested that distinct substrate and inhibitor selectivity of the latter can be attributed mainly to a larger void at the active center and to a local structural modification of the active center environment (*8*, *9*, *12*, *21*, *22*, *25*, *26*). However, this widely accepted view seems to be inconsistent with the finding that although the F295L AChE is almost as reactive as BChE toward butyrylthiocholine (BTC), its corresponding reactivity toward acetylthiocholine (ATC) is reduced relative to either wild-type AChE or BChE (*8*, *17*). Further modification of the HuAChE acyl pocket, mimicking the composition in the HuBChE acyl pocket (the F295L/F297V enzyme), results in reactivity decrease toward both ATC and BTC compared to the F295L HuAChE (*8*). In addition, recent examination of the stereoselectivity of the phosphonylation reaction of HuAChE active center mutants with soman isomers suggests that although the AChE acyl pocket is an important determinant of the relative reactivity toward the P_S- and the P_R-diastereomers, the actual reactivity profiles of the acyl pocket mutant HuAChE, F295L/F297V, and the equine BChE toward soman are quite different (*27*).

In AChE, residues Tyr72(70), Tyr124(121), and Trp286-(279) are localized at or near the rim of the active center gorge and together with Asp74(72) and Tyr341(334) were shown to constitute the peripheral anionic subsite(s) (PAS) (*10*, *11*, *16*, *17*). In BChE positions corresponding to 72, 124, and 286 are substituted by aliphatic amino acids, and consequently this enzyme is less reactive toward bisquaternary inhibitors such as ambenonium and BW284C51, which bind to both the active center and the PAS or toward the PAS specific ligand fasciculin (*9*, *17*, *28*). Thus, the absence of aromatic residues at these positions makes the existence of a PAS on BChE questionable. Yet, affinity of BChE toward the peripheral ligand propidium was shown to be much higher than that of the MoAChE (Y72N/Y124Q/W286A) triple PAS mutant (*17*). These studies as well as photoaffinity labeling studies (*29*, *30*) suggest that the ligand may bind at different loci in AChE and BChE. Thus the marked difference in affinities between AChE and BChE toward PAS ligands may not be related only to the absence of the three aromatic residues from the rim of the gorge (*31*). Moreover, the possible difference in the location of the PAS sites may be related also to the finding that modulation of catalytic activity at high substrate concentration, which is thought to involve substrate binding at the periphery, appears to be different for the two enzymes, leading to substrate inhibition in AChE (*16*, *32*, *33*) and substrate activation in BChE (*31*, *34*−*36*).

In the present study, we further explore the differences between the functional architectures of AChE and BChE active centers by systematic replacements of the relevant aromatic residues along the HuAChE active center gorge. Through comparison of the reactivities of single and multiple mutants toward noncovalent inhibitors, we find that indeed the general architecture of the hexa-HuAChE mutant mimics the more spacious active center of BChE. Yet reactivities of the hexamutant toward certain covalent ligands such as substrates, transition state analogues, and phosphonates reveal a significant functional impairment in the modified enzyme.

MATERIALS AND METHODS

Enzymes, Reagents, and Inhibitors. Mutagenesis of AChE was performed by DNA cassette replacement into a series of HuAChE sequence variants, which conserve the wild-type coding specificity (*37*) but carry new unique restriction sites (*38*−*40*). Generation of mutants W286A(Trp279), F295L(Phe288), F297V(Phe290), and Y337A(Phe330) and the double mutant F295L/F297V was described previously (*8*). Substitution of residues Y72N(Tyr70) and Y124Q-(Tyr121) was carried out by replacement of the *Acc*I−*Nru*I and the *Nru*I−*Nar*I DNA fragments of the AChE-w4 variant (*40*) with synthetic DNA duplexes, respectively. Generation of the double mutant Y72N/Y124Q was carried out by replacements of the *Acc*I-*Dde*I as well as the *Dde*I−*Bst*EII DNA fragments of the AChE-w3 variant (*40*) with the respective fragments from the Y72N and Y124Q variants. The triple mutant Y72N/Y124Q/W286A was generated by inserting the *Eco*RV−*Bst*EII fragment carrying Y72N/Y124Q mutations into the W286A AChE cDNA variant. The triple mutant F295L/F297V/Y337A was generated by replacement of the *Sal*I−*Dde*I as well as the *Dde*I−*Bsu*36I DNA fragments of the neo-cat HuAChE expression vector (*41*) with the respective fragments from the F295L/F297V and Y337A variants of the AChE-w7 vector (*16*). Construction of the hexamutant was carried out by ligation of the relevant DNA fragments from the two triple mutant variants (Y72N/Y124Q/W286A and F295L/F297V/Y337A), resulting in a DNA containing all six mutations (Y72N/Y124Q/W286A/F295L/F297V/Y337A), bounded by two unique restriction sites (*Eco*RV and *Bsu*36I) of the neo-cat vector (*41*). On the basis of previously published genomic sequences of human BChE (*42*, *43*), the complete coding cDNA sequence of BChE was reconstructed through ligation of PCR amplified exons. The full-length cDNA was inserted between the *Eco*RV−*Sal*I sites, replacing the HuAChE sequences in the neo-cat expression vector (*41*).

The sequences of all clones were verified by the ABI PRISM BigDye terminator reaction kit, using the ABI310 genetic analyzer (Applied Biosystems).

Procedures of transfection of the human embryonal kidney-derived cell line (HEK-293) with expression vectors of recombinant enzymes (HuAChEs and HuBChE) and the generation of stable cell clones, expressing high levels of

[2] Amino acids and numbers refer to HuAChE, and the numbers in parentheses refer to the positions of analogous residues in TcAChE according to the recommended nomenclature (*71*).

Scheme 1

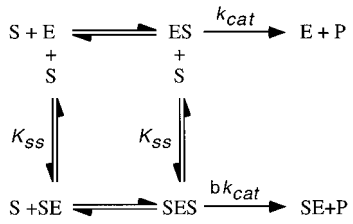

each of the various recombinant products, were described previously (*38*−*40*).

Acetylthiocholine iodide (ATC), butyrylthiocholine iodide (BTC), 5,5′-dithiobis(2-nitrobenzoic acid) (DTNB), ethyl-(*m*-hydroxyphenyl)dimethylammonium chloride (edrophonium), di(*p*-allyl-*N*-dimethylaminophenyl)pentan-3-one (BW284C51), 1,10-bis(trimethylammonium)decane (decamethonium), 9-amino-1,2,3,4-tetrahydroacridine hydrochloride hydrate (tacrine), and diisopropyl phosphorofluoridate (DFP) were purchased from Sigma. Synthetic (±)-huperzine A was obtained from Calbiochem. *m*-(*N*,*N*,*N*-Trimethylammonio)trifluoroacetophenone (TMTFA) was prepared according to the procedure described by Nair et al. (*44*).

Preparation of the racemic mixtures (*45*) of 2-butyl (IBMPF) and 1,2,2-trimethylpropyl (soman) methylphosphonofluoridates followed an accepted procedure using methylphosphonodifluoride and the appropriate alcohol. The PsC*s*-soman stereomer was prepared and purified as described before (*27*, *46*).

Determination of HuAChE Activity and Analysis of Kinetic Data. Activity of HuAChE enzymes was assayed according to Ellman et al. (*47*) (in the presence of 0.1 mg/mL BSA, 0.3 mM DTNB, 50 mM sodium phosphate buffer, pH 8.0, and various concentrations of ATC or BTC), carried out at 27 °C, and monitored by a Thermomax microplate reader (Molecular Devices). Enzyme concentration was determined by ELISA (*40*) and by active site titration (*38*) using the PsC*s*-soman stereomer.

Michaelis−Menten constants (K_m) and the apparent first-order rate constants k_{cat} were determined according to the kinetic treatment described before (*16*, *40*). The apparent bimolecular rate constants k_{app} were calculated from the ratio k_{cat}/K_m. The behavior of either inhibition or activation at high substrate concentration can be described by Scheme 1 in which substrate molecule (S) binds to two different sites (*17*). The dissociation constant for SE is K_{ss} and for SES is αK_{ss}, where $\alpha = 1$. Assuming that S binds to both E and ES, the parameter b reflects the efficiency with which the ternary complex SES forms product. If $0 < b < 1$, there is substrate inhibition; if $b > 1$, there is substrate activation; and if $b = 1$, the enzyme is said to have Michaelian behavior. K_m, K_{ss}, V_{max}, and b were calculated by nonlinear curve fitting of eq 1, using PRISM software (Graphpad).

$$v = \left(\frac{1 + b[S]/K_{ss}}{1 + [S]/K_{ss}}\right)\left(\frac{V_{max}}{1 + K_m[S]}\right) \quad (1)$$

Values of competitive inhibition constants (K_i) for the noncovalent inhibitors edrophonium, tacrine, huperzine A, BW284C51, and decamethonium were determined from the effects of various concentrations of the inhibitor on K_m and V_{max} of the enzyme-catalyzed hydrolysis of ATC. All the HuAChE enzymes examined formed rapid equilibria with the inhibitors, allowing for an immediate addition of increasing amounts of ATC to the enzyme−inhibitor mixture (preincubation of the enzymes with huperzine A for 10 min, before addition of the substrate, or simultaneous mixing yielded the same results). The values of K_i were computed from the secondary plots of the apparent values of K_m (slopes of $1/V$ vs $1/[S]$) vs concentrations of the respective inhibitors as described before (*8*).

The apparent first-order rate constants for the time-dependent inhibition of the wild-type HuAChE mutants by TMTFA were determined by periodical measurement of the initial rate of substrate hydrolysis of aliquots taken from the reaction mixture. Following the kinetic treatment described by Nair et al. (*44*, *48*) and assuming a two-state inhibition mechanism, the values of k_{on} and k_{off} could be estimated from the linear plots of k_{obs} vs inhibitor concentration, according to the equation:

$$k_{obs} = k'_{on}[TMTFA] + k_{off} \quad (2)$$

Since in aqueous solution TMTFA is a mixture of the free ketone ($TMTFA_{ket}$) and the ketone hydrate ($TMTFA_{hyd}$), corrected values of the association rate constants were obtained from $k_{on} = k'_{on}(1 + [TMTFA_{hyd}]/[TMTFA_{ket}])$, using the ratio of hydrated and ketone forms of TMTFA (62500) as determined by ^{19}F NMR (see ref *44*). Direct measurements of k_{off} for wild-type HuAChE, its hexamutant, and HuBChE were determined from the rates of regeneration of enzymatic activity following removal of excess of free inhibitor by filtration through Centrisart C-4 microcentrifuge filters (Sartorius). The measured k_{off} values were in a good agreement with the calculated values.

Measurements of phosphylation rates, with HuAChE and its mutants, were carried out in at least four different concentrations of DFP, soman, and IBMPF (I), and residual enzyme activity (E), at various time points, was monitored. The apparent bimolecular phosphylation rate constants (k_i), determined under pseudo-first-order conditions, were computed from the slopes of the plots of $\ln(E)$ vs time at different inhibitor concentrations. Rate constants under second-order conditions were determined from plots of $\ln\{E/[I_0 - (E_0 - E)]\}$ versus time (*27*). Stereoselectivity of the enzymes toward various phosphonates was determined by active site titrations, comparing residual activities of enzymes inhibited by the appropriate racemic phosphonate to that of soman stereomer PsC*s* (*49*).

Molecular Dynamics Simulation. All simulations were performed on an Octane Silicon Graphics workstation using the Dynamics execution and analysis modules of SYBYL 6.6 (Tripos, 1999). An AMBER all-atom parameter set was used throughout the simulations. The starting conformation of the wild-type enzyme was obtained from the X-ray structure of the HuAChE−fasciculin complex model (*3*, structure 1b41 on the Protein Data Bank) by removal of the ligand and relaxation of the contact regions. The essential water molecules W659 and W670 (*3*) were retained throughout the simulations. Models of the HuAChE mutants were obtained by relaxation of the appropriately modified structures. One hundred and forty-seven residues were involved

Table 1: Kinetic Parameters[a] of Hydrolysis of Acetylthiocholine and Butyrylthiocholine by HuBChE, HuAChE, and Its Mutants

	ATC			BTC		
type	K_m (mM)	k_{cat} ($\times 10^{-5}$ min^{-1})	k_{cat}/K_m ($\times 10^{-8}$ M^{-1}·min^{-1})	K_m (mM)	k_{cat} ($\times 10^{-5}$ min^{-1})	k_{cat}/K_m ($\times 10^{-8}$ M^{-1}·min^{-1})
HuAChE						
wild type	0.14	4.0	29	0.30	0.08	0.3
Y72N	0.14	5.4	38	0.14	0.09	0.7
Y124Q	0.19	4.5	24	0.16	0.25	1.5
W286A	0.25	4.1	16	0.20	0.27	1.4
F295L	0.25	1.0	4	0.04	0.26	6.5
F297V	0.78	1.5	1.9	0.25	0.60	2.7
Y337A	0.09	1.4	16	0.24	0.03	0.1
Y72N/Y124Q	0.14	4.1	29	0.25	0.20	0.8
F295L/F297V	1.3	0.5	0.4	0.42	0.43	1.2
Y72N/Y124Q/W286A	0.26	4.7	18	0.20	0.19	1.0
F295L/F297V/Y337A	2.9	0.8	0.3	0.90	0.55	0.6
Y72N/Y124Q/W286A/ F295L/F297V/Y337A	4.7	0.8	0.2	3.3	1.5	0.5
HuBChE	0.04	0.5	13	0.05	1.1	22

[a] Values represent means of triplicate determinations with standard deviation not exceeding 20%.

in the simulation. Initial equilibrations at 3000 K (20 ps) were followed by 160 ps of dynamics runs at 4000 K with constrained main chain.

RESULTS

According to the molecular models of BChE proposed in the past (*12*, *50*), out of about 30 residues lining the active site gorge, only 10 amino acids differ between HuAChE and HuBChE. Six of these changes involve substitutions of aromatic residues in HuAChE by nonaromatic residues in HuBChE [the other four, V73I(71), S125T(122), L289V-(282), and S293T(286), being conservative replacements]. To further investigate whether this diminished "aromatic lining" of the BChE active site gorge is the main determinant of its distinct ligand selectivity, a HuAChE enzyme carrying appropriate replacements of all of the six aromatic residues has been generated (Y72N/Y124Q/W286A/F295L/F297V/Y337A). In addition, triple HuAChE mutants, with BChE-like replacements at the active center (F295L/F297V/Y337A) and the peripheral site (Y72N/Y124Q/W286A), were constructed. These multiple HuAChE mutants, together with the previously examined HuAChE derivatives carrying double and single aromatic residue replacements, were used to examine whether gradual "butyrylization" of HuAChE leads to increasingly BChE-like reactivity characteristics toward substrates and noncovalent and covalent inhibitors shown in Figure 1.

Hydrolytic Activity toward ATC and BTC. As already observed in the past wild-type HuAChE and HuBChE display similar reactivity toward ATC, with bimolecular rate constants of 2.9×10^9 and 1.3×10^9 M^{-1}·min^{-1}, respectively (see Table 1). No significant substrate selectivity of HuBChE is evident with respect to ATC and BTC, as the corresponding values of K_m and k_{cat} are similar for both substrates. On the other hand, HuAChE displays nearly 100-fold selectivity for ATC over BTC, with most of this reactivity decrease originating from the 50-fold difference between the corresponding values of k_{cat} (see Table 1).

The hexamutant HuAChE (Y72N/Y124Q/W286A/F295L/F297V/Y337A) exhibits low catalytic activity toward both ATC and BTC with bimolecular rate constants of 2×10^7 and 5×10^7 M^{-1}·min^{-1}, respectively (see Table 1). In fact,

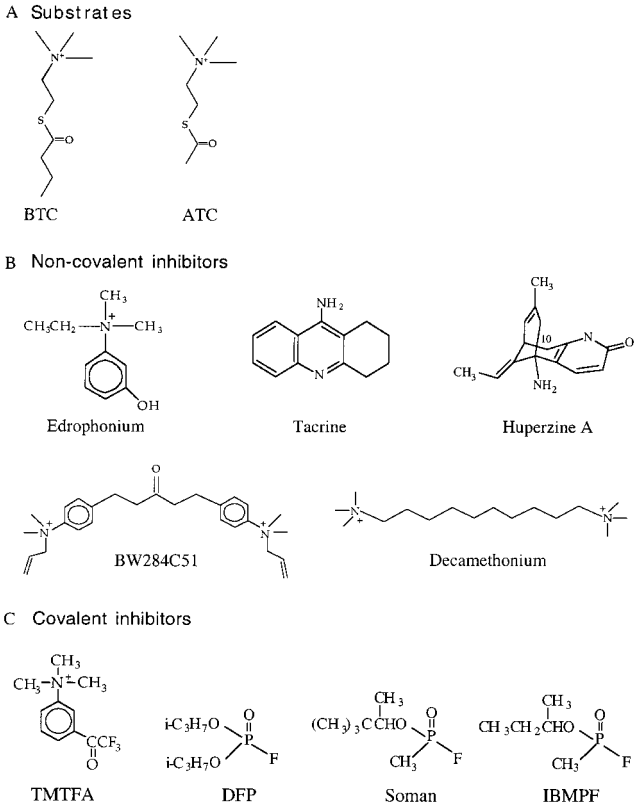

FIGURE 1: Chemical formulas of ligands used in this study.

catalytic activities (k_{app}) of the hexamutant HuAChE for ATC and BTC are approximately 65- and 45-fold lower, respectively, than the corresponding values of HuBChE. It appears that this large difference in reactivity between the hexamutant and HuBChE is mainly associated with an increase in K_m values (4.7 mM vs 0.04 mM for ATC and 3.3 mM vs 0.05 mM for BTC). We note also that K_m values for both BTC and ATC of hexamutant HuAChE are higher (10−30-fold) than those determined for the wild-type HuAChE enzyme. Furthermore, the k_{cat} values for hydrolysis of substrates by the hexamutant appear to be also affected relative to the wild-type enzyme. For ATC we find a slight decrease (5-fold) but for BTC an increase (approximately 20-fold) in k_{cat} values relative to HuAChE.

The reactivity characteristics of the hexamutant HuAChE toward ATC are fully reproduced in the F295L/F297V/Y337A HuAChE and to a lesser extent in the double mutant F295L/F297V. For both of these triple and double mutant enzymes a 9−20-fold increase of the K_m values and a 5−8-fold decrease of the k_{cat} values relative to the wild-type HuAChE were observed. The hexamutant HuAChE and the triple and double active center mutants also display similar catalytic activities toward BTC. The observation that reactivity toward substrates is determined predominantly by mutations at the active center is consistent with the lack of corresponding effects due to the multiple mutations at the PAS. Thus, the catalytic activities of the triple PAS mutant Y72N/Y124Q/W286A HuAChE toward ATC and BTC are comparable to those of the wild-type enzyme.

In conclusion, with respect to ATC the values of the bimolecular rate constants (k_{app}) of the hexamutant or the F295L/F297V/Y337A HuAChEs are about 2 orders of magnitude lower than those of either the wild-type HuAChE or the HuBChE enzymes. For BTC the values of k_{app} for these hexamutant and triple mutant HuAChEs are comparable to those of the wild-type HuAChE and accordingly about 40-fold lower than that of HuBChE.

Substrate Inhibition. Hydrolytic activities of HuAChE and HuBChE show different dependence on substrate concentration, with the former exhibiting substrate inhibition at [ATC] > 2 mM, while for the latter, substrate activation has been reported at a BTC concentration range of 20−40 mM and substrate inhibition at [BTC] > 40 mM (*31*, *51*). Effects of excess substrate on hydrolytic activity of HuAChE enzymes carrying single and multiple replacements of aromatic residues along the active site gorge were examined according to a kinetic model depicted in Scheme 1. The experimental values of factor *b* (see Scheme 1) are a measure of relative activity of the complexes ES and SES ($b > 1$ demonstrates substrate activation while $b < 1$ demonstrates substrate inhibition).

As already shown before (*16*, *17*), single replacement of residues Tyr72, Tyr124, and Trp286 at the periphery and of residue Phe295 at the active center affects secondary ATC binding to the enzyme (reflected in the values of K_{ss}) but has no effect on corresponding values of factor *b* (see Table 2). On the other hand, replacements of residues Phe297 and Tyr337 abolished substrate inhibition by ATC (*9*, *16*). Unlike the case of ATC, the secondary binding constant of BTC to the Y72N enzyme resembles that of the wild-type HuAChE. In addition, substrate inhibition by excess of BTC is not abolished by replacement of Phe297.

In the case of the F295L/F297V and the F295L/F297V/Y337A HuAChE mutants no substrate inhibition could be observed for both ATC and BTC (see Table 2; $b = 1.0$). The hexamutant HuAChE is also insensitive to substrate inhibition by ATC and BTC, at the concentration range tested, with similar *b* values. Notably, none of the mutant HuAChE enzymes exhibited a switch from substrate inhibition to substrate activation. In MoAChE substrate activation has been reported for the F297I enzyme (*17*). Thus it appears that the structural features distinguishing between AChE and BChE with respect to substrate inhibition/activation are not dependent only on the aromatic residues lining the respective active site gorge. This observation is consistent with the *b* values (see eq 1) reported for BChE mutants where aromatic residues have been introduced to mimic the AChE sequence (*25*, *35*). In these cases substrate activation persisted in analogy to the wild-type BChE.

Table 2: Kinetic Parameters[a] for Substrate Inhibition/Activation of HuBChE, HuAChE, and Its Mutants

	ATC		BTC	
type	K_{ss} (mM)	*b*	K_{ss} (mM)	*b*
HuAChE				
wild type	6 ± 1	0.2 ± 0.02	3 ± 1	0.4 ± 0.1
Y72N	21 ± 8	0.3 ± 0.1	2 ± 0.6	0.5 ± 0.1
Y124Q	15 ± 3	0.2 ± 0.1	11 ± 3	0.1 ± 0.1
W286A	16 ± 8	0.3 ± 0.1	30 ± 10	0.4 ± 0.1
F295L	28 ± 3	0.3 ± 0.1	20 ± 2	0.1 ± 0.02
F297V	1 ± 0.5	0.9 ± 0.1	50 ± 10	0.4 ± 0.1
Y337A		0.9 ± 0.2	8 ± 2	0.8 ± 0.1
Y72N/Y124Q	20 ± 7	0.3 ± 0.1	24 ± 4	0.1 ± 0.1
F295L/F297V		1.0 ± 0.1		1.0 ± 0.1
Y72N/Y124Q/W286A	15 ± 2	0.5 ± 0.1	20 ± 5	0.5 ± 0.2
F295L/F297V/Y337A		1.0 ± 0.1		1.0 ± 0.2
Y72N/Y124Q/W286A/F295L/F297V/Y337A		0.9 ± 0.2		1.0 ± 0.1
HuBChE	4 ± 1	1.9 ± 0.2	1 ± 0.2	2.4 ± 0.2

[a] The kinetic parameters were determined according to eq 1 (see Materials and Methods).

Reactivity toward the AChE Transition State Analogue TMTFA. The kinetics of AChE inhibition by TMTFA has been studied extensively since the AChE−TMTFA tetrahedral covalent adduct is believed to resemble the transition state of the acylation process (*44*, *48*, *52*). On the other hand, only very recently a comparable reaction with BChE has been described (*53*). Thus, comparison of TMTFA reactivities toward the wild-type and certain mutant HuAChEs as well as HuBChE could shed new light on the effects of structural differences in the active center gorge on accommodating and covalently binding of substrates.

TMTFA was found to be a time-dependent inhibitor of HuAChE and its mutants, as well as of HuBChE, showing linear dependence of the pseudo-first-order rate constants of inhibition (k_{obs}) on inhibitor concentrations (*44*, *48*). The bimolecular rate constants k_{on} and the dissociation rate constants k_{off} were calculated from the relation $k_{obs} = k_{on}[TMTFA] + k_{off}$ and corrected for hydration of the free ketone (see Materials and Methods). Values of k_{off} for the different enzymes were also determined directly by monitoring the regeneration of hydrolytic activity from the corresponding adducts and found to be in good agreement with those determined according to the above equation (see Table 3).

Comparison of TMTFA reactivities toward wild-type HuAChE and toward HuBChE shows that while the values of k_{on} are practically equivalent (1.9×10^{11} and 1.7×10^{11} $M^{-1}\cdot min^{-1}$, respectively), the dissociation rate constant (k_{off}) of the HuBChE−TMTFA adduct is 66-fold higher than that of the corresponding HuAChE conjugate (see Table 3). The value of k_{on} for TMTFA inhibition of the hexamutant HuAChE is 170-fold lower than that of HuBChE, and the corresponding value of k_{off} is 13-fold lower. Thus, butyrylization of the HuAChE active center both fails to reconstitute the functional environment of HuBChE necessary for high reactivity toward TMTFA and impairs the corresponding functional architecture of HuAChE. While most of the

Table 3: Inhibition Rate Constants of HuBChE, HuAChE, and Its Mutants by the Transition State Analogue TMTFA

type	TMTFA k_{on}[a] ($\times 10^{-9}$ $M^{-1}\cdot min^{-1}$)	TMTFA k_{off}[a] ($\times 10^{4}$ min^{-1})	TMTFA rel k_{on} (WT/mutant)	ATC rel k_{app}[c] (WT/mutant)
HuAChE				
wild type	190	6[b]	1	1
Y337A	250	5	0.8	1.8
F295L/F297V	4	20	50	73
Y72N/Y124Q/W286A	63	25	3	1.6
F295L/F297V/Y337A	6	55	32	97
Y72N/Y124Q/W286A/F295L/F297V/Y337A	1	30[b]	190	145
HuBChE	170	400[b]	1.1	2.2

[a] Values of k_{on} and k_{off} were determined from the slope and intercept, respectively, of the plots of k_{obs} vs five different concentrations of inhibitor (spanning the range of 1 order of magnitude) of [TMTFA], with correlation coefficients of at least 0.95 (see Materials and Methods). [b] Values of k_{off} were determined from the rates of regeneration of hydrolytic activity following removal of the free inhibitor: WT HuAChE $= 4 \times 10^{-4}$ min^{-1}, Y72N/Y124Q/W286A/F295L/F297V/Y337A $= 40 \times 10^{-4}$ min^{-1}, and HuBChE $= 300 \times 10^{-4}$ min^{-1}. [c] Values are according to results depicted in Table 1.

impairment is due to mutations at the HuAChE acyl pocket (see Table 3), a small effect due to modifications at the PAS could be observed (the value of k_{on} for the Y72N/Y124Q/W286A HuAChE is 3-fold lower than that for the wild-type enzyme). Therefore, the 190-fold decrease in the value of k_{on} for the hexamutant HuAChE, relative to that of the wild-type enzyme, results predominantly from the triple replacements at the active center.

Multiple mutations at the HuAChE active center gorge appear to decrease the stability of the corresponding HuAChE−TMTFA conjugates (see Table 3). Yet the value of k_{off} for the hexamutant conjugate is merely 5-fold higher than that for the wild-type HuAChE (and 13-fold lower than that for HuBChE), suggesting again that the active center environments participating in stabilization of the TMTFA tetrahedral intermediates with HuBChE and with hexamutant HuAChE are quite different.

Reactivity toward Organophosphate Inhibitors. While reactions of AChE with substrates and with TMTFA involve rapid formation of covalent tetrahedral intermediates, interaction of ChEs with organophosphate inhibitors such as soman, IBMPF, or DFP is thought to involve initial formation of a noncovalent complex with the tetrahedral species (*22*, *54*, *55*). Thus the inhibitory activity of these agents may further probe the influence of a modified AChE active center environment on the emergence of tetrahedral intermediates in reactions with substrates.

Reactivities of the bulky phosphate DFP toward the hexamutant HuAChE and toward HuBChE were found to be very similar and 150−166-fold higher than the corresponding activity toward the wild-type HuAChE (Table 4). This reactivity enhancement toward DFP may result from the space-creating replacements at the acyl pocket (*22*) as well as from the replacements at the PAS. These findings are consistent with the recently reported X-ray structure of an aged AChE−DFP conjugate, where both the acyl pocket and part of the PAS seem distorted due to interaction with the phosphoryl isopropoxy substituent (*56*). The notion that space-creating mutations at both the HuAChE acyl pocket and the PAS result in a HuBChE-like binding environment for the bulky phosphoryl substituents is consistent also with the stoichiometry of the hexamutant phosphonylation by racemic methylphosphonates. While the stoichiometry of reactions of HuBChE with racemic soman and IBMPF is 1:1 (indicating a relatively low stereoselectivity of this enzyme toward the corresponding phosphonate Ps-diastereomers), equivalent reactions of both the wild-type and the F295L/F297V/Y337A HuAChEs display 2:1 stoichiometry (see Figure 2). However, reaction of the hexamutant HuAChE with IBMPF proceeds with 1:1 stoichiometry, indicating that the respective stereoselectivity of this enzyme is lower than that of the F295L/F297V/Y337A HuAChE and may in fact be similar to that of HuBChE. Yet, the acyl pockets of HuBChE and of hexamutant HuAChE are not structurally equivalent, as indicated by the fact that the latter still displays 2:1 stoichiometry in reaction with the somewhat bulkier soman (see Figure 2).

Table 4: Kinetic Constants[a] of Phosphylation Reactions of HuBChE, HuAChE, and Its Mutants by DFP, Soman, and IBMPF

type	k_i ($\times 10^{-4}$ M^{-1} min^{-1}) DFP	soman	IBMPF
HuAChE			
wild type	10 (1)[b]	10000 (1)	13000 (1)
Y72N/Y124Q	16 (0.6)	11000 (1)	15000 (1)
F295L/F297V	800 (0.01)	280 (36)	500 (26)
Y72N/Y124Q/W286A	30 (0.3)	13300 (0.8)	18000 (0.7)
F295L/F297V/Y337A	150 (0.07)	120 (85)	100 (130)
Y72N/Y124Q/W286A/F295L/F297V/Y337A	1500 (0.01)	50 (200)	290[c] (45)
HuBChE	1660 (0.01)	4000[c] (2.5)	4000[c] (3)

[a] Values were determined with five different concentrations of inhibitor (spanning the range of 1 order of magnitude) with the standard deviation not exceeding 20%. [b] The number in parentheses represents the ratio between the rate constant of WT HuAChE to that of the rate constant of the corresponding mutant. [c] Stoichiometry ratio of 1:1 was obtained by active site titration for the indicated mutants (for all other enzymes the stoichiometry ratio was 1:2).

In contrast to the nearly equivalent reactivities of the hexamutant HuAChE and the HuBChE toward DFP, the corresponding reactivities toward the two methylphosphonates soman and IBMPF were surprisingly different. For these organophosphate inhibitors we find a decrease in the hexamutant reactivity of 80−14-fold relative to HuBChE (note that corresponding decrease in reactivity relative to the wild-type HuAChE is even greater; see Table 4). While affinities of HuAChE enzymes carrying replacements at the PAS toward the two methylphosphonates resemble those of the wild-type enzyme, replacements at the active center result in 40−80- and 30−130-fold drops in the corresponding affinity for the F295L/F297V and the F295L/F297V/Y337A HuAChEs toward soman and IBMPF, respectively. These

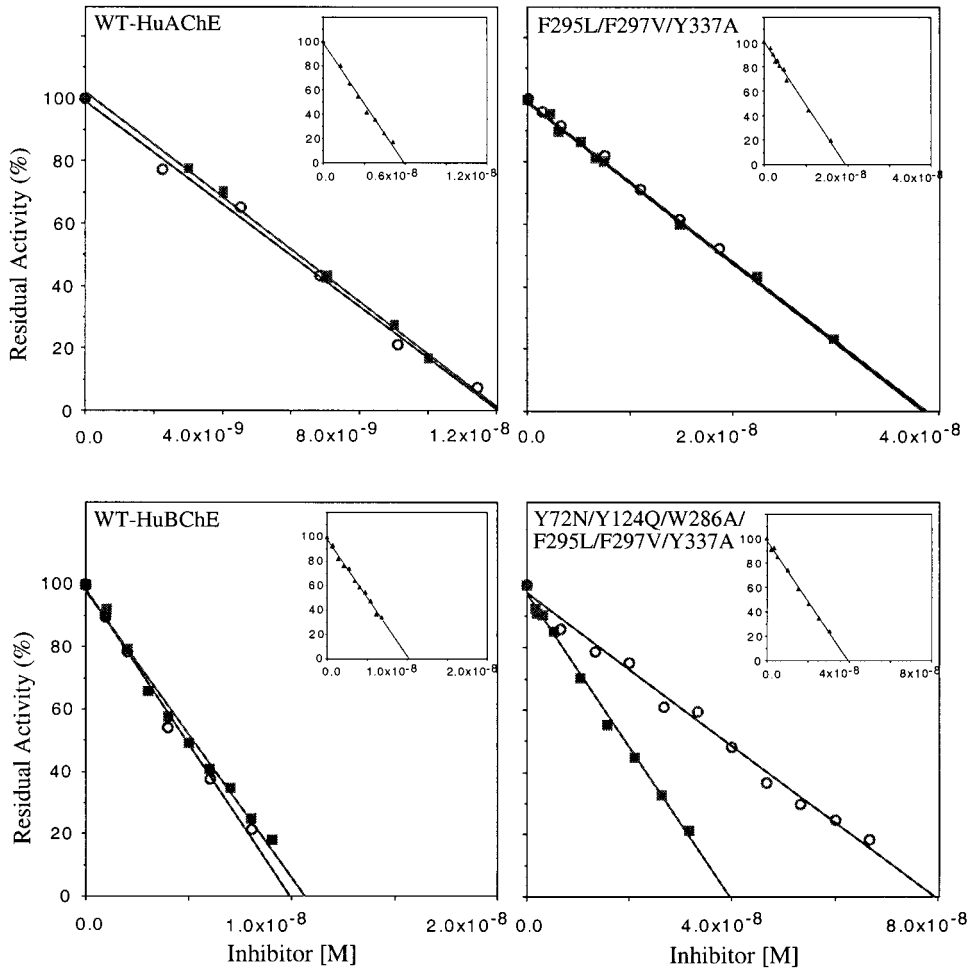

FIGURE 2: Comparison of active site titration profiles of HuAChE, the triple active center mutant F295L/F297V/Y337A, the hexamutant of HuAChE, and HuBChE with soman and IBMPF. For each enzyme preparation the active site concentration was determined using the PsCs-soman stereomer which reacts in all cases with 1:1 stoichiometry (see inset). For both racemic soman (○) and racemic IBMPF (■) the wild-type HuAChE and its triple mutant display approximate stoichiometric ratios of 2:1 while the HuBChE exhibits a ratio of 1:1. In the case of the hexamutant of HuAChE the stoichiometric ratios for racemic soman and IBMPF are 2:1 and 1:1, respectively.

results indicate that the relative destabilization of the hexamutant HuAChE−methylphosphonate complexes (15−200-fold as compared to wild-type HuAChE or to HuBChE) is entirely due to mutations at the active center. These observations cannot be rationalized by an inferior accommodation of the phosphonyl methyl substituent in the more spacious acyl pocket, since a similarly composed acyl pocket in the HuBChE does not produce the same effect. Thus, unlike the case of DFP, accommodation of tetrahedral species with lower steric demands at the active center acyl pocket seems to be different for the hexamutant HuAChE and for HuBChE. This difference appears to be common to the various tetrahedral species formed in the AChE active center either by noncovalent binding (methylphosphonates such as soman or IBMPF) or through formation of covalent intermediates (substrates, TMFTA).

Reactivity toward Noncovalent Inhibitors. The functional architecture of HuAChE enzymes carrying multiple replacements of aromatic residues at the active center gorge and its possible resemblance to that of BChE were further investigated through interactions with noncovalent inhibitors. Prototypical active center ligands such as edrophonium, tacrine, and huperzine A, as well as BW284C51 and decamethonium, the ligands bridging the active center and the PAS, were used to probe the changes in affinity resulting from removal of aromatic residues from the previously defined binding subsites (*8*, *10*; see Table 5).

(a) Edrophonium. Examination of the effects of single replacements of aromatic residues at the active center on enzyme reactivity toward edrophonium (*10*, *57*) indicated that only substitutions of Tyr337 and Phe297 by aliphatic residues had some effect on binding (8-fold and 6-fold, respectively). The loss of reactivity toward edrophonium, observed for the hexamutant HuAChE, is 170-fold compared to the wild-type HuAChE, and its inhibition constant is equivalent to that measured for HuBChE (Table 5). We note that most of this effect is contributed by the combined replacements of all of the three aromatic residues at the active center, as manifested by the fact that the measured values of K_i for the F295L/F297V/Y337A and the Y72N/Y124Q/W286A HuAChEs are 53 μM and 1.1 μM, respectively, while that of HuBChE is 50 μM.

(b) Tacrine. Previous studies with this active center inhibitor have shown that its binding is affected predominantly by residues of the HuAChE "aromatic patch" (Trp86, Tyr133, Tyr337) (*23*). In particular, replacement of the aromatic residue at position 337 by Ala increased the affinity of the resulting mouse (*17*) and human (*23*) AChEs toward tacrine and could partially account for the higher affinity of tacrine toward BChE (*15*, *49*). Residue Tyr337 is substituted

Table 5: Inhibition Constants[a] of HuBChE, HuAChE, and Its Mutants by Noncovalent Ligands

type	edrophonium K_i (μM)	huperzine A K_i (nM)	tacrine K_i (nM)	decamethonium K_i (μM)	BW284C51 K_i (nM)
HuAChE					
wild type	0.3	16	57	4.6	10
Y72N/Y124Q	1.1	90	55	200	270
F295L/F297V	2.2	50	60	210	55
Y72N/Y124Q/W286A	1.1	30	35	260	8000
F295L/F297V/Y337A	53	20000	9	210	920
Y72N/Y124Q/W286A/ F295L/F297V/Y337A	50	400000	12	360	170000
HuBChE	50	50000	12	2.5	14000

[a] Values were determined with five different concentrations of inhibitor (spanning the range of 1 order of magnitude) with the standard deviation not exceeding 20%.

also in the multiple active center mutant HuAChEs (F295L/F297V/Y337A and hexamutant) and is probably contributing to the minor 5-fold increase in affinity of these enzymes for tacrine. Moreover, the values of dissociation constants for tacrine complexes with these HuAChE enzymes are practically equivalent to that with HuBChE (Table 5). This again suggests that the active center regions of the hexamutant HuAChE, probed by ligands such as tacrine, are quite similar to those in HuBChE. As could be expected from previous studies (*23*), replacement of aromatic residues at the PAS has no effect on tacrine binding.

(c) Huperzine A. HuAChE reactivity toward this bulky inhibitor was previously shown to be affected significantly by replacements of active center residues which did not seem to be directly involved in the accommodation of this ligand (*23*, *52*). This may be exemplified by the large effects of mutation of the oxyanion hole residue Gly121 or the adjacent residue Gly122 on huperzine A binding (*52*). Therefore, the relatively minor effects due to single replacements of aromatic residues at the active center or the PAS are difficult to explain in terms of specific interactions with the ligand. The exception is residue Tyr337, the replacement of which has been long known to lower affinity toward huperzine A (*58*, *59*), probably due to loss of cation$-\pi$ interaction with the ligand amine moiety (*23*). Thus, the 1250-fold drop in affinity toward huperzine A of the F295L/F297V/Y337A HuAChE (Table 5), as compared to the wild-type enzyme, seems to result mostly from the replacement at position 337. However, since replacements of aromatic residues at the PAS do not seem to affect reactivity toward huperzine A (e.g., Y72N/Y124Q/W286A HuAChE; see Table 5), the structural basis for the further decrease in affinity of the hexamutant toward this ligand is unclear. In any case, the dissociation constant of the huperzine A−hexamutant HuAChE complex is 25 000-fold higher than that of wild-type HuAChE and only 8-fold higher than that of the corresponding complex with HuBChE. This underscores the similarity of the molecular environments of the hexa-HuAChE mutant and HuBChE as sampled by this ligand.

(d) BW284C51. This bisquaternary ligand has long been known to display an over 3 orders of magnitude selectivity toward AChEs as compared to BChE (*54*). It binds along the AChE active site gorge spanning the binding sites at the active center and the PAS (*10*, *60*). Indeed, the affinity of HuAChE enzymes toward this inhibitor is affected by perturbations at both the active center and the PAS with affinity decreases of 800-fold and 92-fold for Y72N/Y124Q/W286A and F295L/F297V/Y337A HuAChEs, respectively. The corresponding affinity of the hexamutant HuAChE seems to reflect approximately the contributions of the structural changes at the two binding subsites. The hexamutant HuAChE is about 12-fold less reactive toward BW284C51 than the HuBChE. Since the structural motif of BW284C51 interacting with the AChE active center resembles edrophonium (*10*), we may assume that the modified HuAChE active center and the active center of HuBChE contribute similarly to the overall affinity toward the ligand. Therefore, the somewhat different affinities of the hexamutant HuAChE and the HuBChE may originate from minor structural differences, which are not related to aromatic residues, along the active center gorge of the two enzymes.

(e) Decamethonium. This bisquaternary ligand differs from BW284C51 in that it binds essentially with same affinity toward HuAChE and HuBChE (ref *17* and Table 5). Nevertheless and unlike the other noncovalent ligands, the phenotype of the hexamutant is markedly different from that of HuBChE with respect to binding decamethonium. Yet, in line with the fact that this ligand binds to the PAS (*10*, *61*, *62*), it is not surprising to find a substantial decrease in affinity of the Y72N/Y124Q, Y72N/Y124Q/W286A and of the hexamutant HuAChEs toward decamethonium (40-, 60-, and 80-fold, respectively). It is therefore quite clear that the binding modes of decamethonium to HuBChE and to HuAChE are different. In fact, such alternative binding was suggested in an earlier study where binding of decamethonium to BChE was modeled to bridge residues corresponding to Trp86 and Trp236 in AChE, which are well inside the gorge (*17*). However, it appears that mutations at the bottom of the gorge (F295L/F297V and F295L/F297V/Y337A) lead to a *decrease* in affinity toward decamethonium which could not be expected from either the models of the AChE−decamethonium complex (*10*, *17*) or the X-ray structure of TcAChE and MoAChE−decamethonium complexes (*61*, *62*). Finally, the effects of the mutations in the active center and the PAS are not additive, and the various double and triple as well as the hexa-HuAChE mutants have similar inhibition constants for decamethonium (2 orders higher than wild-type HuAChE; Table 5). Thus, although these results reveal some intriguing features with respect to binding of decamethonium to HuAChE, it appears that this ligand is currently not very useful to probe the active center differential characteristics of AChE and BChE.

DISCUSSION

Early sequence comparisons of AChE and BChE combined with the X-ray structure of TcAChE identified three

inhibitor binding regions distinguishing the two enzymes (*63*−*65*). In AChE each of these regions is defined by a cluster of aromatic residues that seem uniquely disposed to accommodate the particular specificity requirements of the inhibitor, while in BChE the equivalent position bears aliphatic residues. One of these regions is located at the entrance to the active site gorge, about 15 Å away from the catalytic serine, and its composition is thought to affect primarily the AChE specificity toward bisquaternary ligands such as BW284C51. The other two regions, the acyl pocket (Phe295, Phe297) and the hydrophobic subsite (containing Tyr337), are integral parts of the active center functional architecture, accommodating differentially ligands specific for AChE and BChE. The effects of residue substitutions at each of these regions have been investigated, mostly by single replacements (*8*−*12*, *16*, *17*, *24*, *25*, *31*), leading to certain conclusions with regard to the structural and functional correspondence between the two cholinesterases: (a) The difference in substrate specificity between AChE and BChE is predominantly due to a more open acyl pocket of the latter, accommodating more readily the larger acyl groups of butyrylcholine or benzoylcholine. (b) The more open acyl pocket is responsible also for BChE specificity toward organophosphorus inhibitors such as iso-OMPA or phosphates such as DFP, DEFP, and paraoxon and for its greatly diminished stereoselectivity toward chiral phosphonates such as soman or IBMPF. (c) BChE selectivity toward tacrine and other aminoacridines as well as toward carbamates like bambuterol is predominantly due to the absence of an aromatic residue at the position equivalent to 337 of the hydrophobic subsite. Other bulky inhibitors such as soman seem to sample similar hydrophobic environments in BChE and AChE. (d) The absence of some aromatic residues at the PAS in BChE is probably responsible for its lower affinity, compared to AChE, toward bisquaternary ligands that bridge the active center and the rim of the gorge, such as BW284C51.

These conclusions are based mainly on single "space-creating" mutations in AChEs as well as on "space-reducing" mutations in BChE and are compatible with the generally accepted notion that interactions of substrates as well as of covalent and noncovalent inhibitors with AChE and BChE reveal nearly equivalent architectures of the respective active centers. Yet as mentioned earlier, reactivity differences of BChE and of certain acyl pocket AChE mutants toward the substrates ATC or BTC (*8*, *9*, *12*) and certain stereoselective alkyl methylphosphonates (*21*, *27*) imply that active centers of AChE and BChE may not be as similar as thought before.

Examination of reactivity of the hexamutant HuAChE toward noncovalent inhibitors seems to indicate that the active center architecture of this enzyme indeed resembles that of HuBChE (Table 5). For the relatively small active center ligands such as edrophonium or tacrine, the ratio of the respective inhibition constants of BChE and hexamutant HuAChE is 1. For the much bulkier huperzine A or the active center and PAS bridging ligand BW284C51, we find that while affinities of the hexamutant are 17 000−25 000-fold lower than those measured for HuAChE, they are only 8−12-fold different from those determined for HuBChE. In particular, affinities of the triple active center mutant F295L/F297V/Y337A toward edrophonium, tacrine, and huperzine A are very similar to those of HuBChE (Table 5). Thus, the multiple replacement of the active center aromatic residues Phe295, Phe297, and Tyr337 of HuAChE by the respective aliphatic residues Leu, Val, and Ala of HuBChE does not affect the overall architecture of the active center but rather creates local voids that seem to be characteristic also to the corresponding architecture of HuBChE. In this modified HuAChE active center the positioning and function of residues, most important for ligand accommodation [like Trp86 or Tyr133 (*57*)], appear unchanged from those in the wild-type HuAChE and HuBChE. Furthermore, it appears that additional replacements of the three aromatic residues at the PAS by aliphatic residues do not seem to affect in a major way the accommodation of these noncovalent ligands at the active center.

In view of this conclusion it was rather surprising to find that the hexamutant HuAChE is about 40−140-fold less efficient than HuBChE or HuAChE, with respect to hydrolysis of both ATC and BTC. Most of the effect can be attributed to replacements of the three aromatic residues at the active center (Phe295, Phe297, and Tyr337). The discrepancy between the capability of the hexamutant HuAChE to accommodate noncovalent ligands in a HuBChE-like fashion and its inferior catalytic activity toward substrates may suggest that elements of the catalytic machinery have been affected by the multiple mutations. Several observations seem to be consistent with such a possibility. Removal of the steric constrains in the acyl pocket of HuAChE by mutation of residue Phe295 to either alanine or leucine imparts BChE-like catalytic activity to HuAChE toward BTC. However, substitution of additional aromatic residues leads to a decline of this activity, and in the hexamutant the catalytic activity toward BTC resembles actually that of the wild-type HuAChE (which is 50-fold lower than that of HuBChE). In addition, although the HuAChE and HuBChE enzymes are almost equally efficient catalysts of ATC hydrolysis, creation of a HuBChE-like void volume in the HuAChE active center lowers very significantly the catalytic activity toward ATC. Finally, the catalytic activity of the hexamutant HuAChE is very similar for ATC and BTC, irrespective of their size difference.

Further demonstration that the aromatic residue replacements affect the HuAChE catalytic machinery, while preserving the overall HuAChE (and HuBChE) active center architecture, is provided by experiments with TMTFA, the prototypical AChE transition state analogue. The TMTFA molecule has been thoroughly investigated with respect to the structure of its tetrahedral adduct with TcAChE (*66*) as well as to the kinetics of its reactions with various wild-type and mutated AChEs (*48*, *52*, *67*). The accepted kinetic model of TMTFA reactivity indicates that the tetrahedral adduct is formed in a single kinetic step, and therefore the corresponding rate constant (k_{on}) is analogous to k_{app} (k_{cat}/K_m) of the catalytic process. Indeed, examination of the relative rate constant values in Table 3 shows analogous response of HuAChE reactivity, toward TMTFA and toward the substrate ATC, that culminates in the 150-fold decrease of k_{app} for the hexamutant HuAChE catalytic activity, as compared to a 190-fold decrease of reactivity toward TMTFA. In addition, a 170-fold ratio of TMTFA k_{on} values for HuBChE and for the hexamutant HuAChE has been observed. Thus it appears that the difference in catalytic activity and in reactivity toward TMTFA, between both wild-

type HuAChE and HuBChE and the hexamutant HuAChE, is in the reduced ability of the latter to accommodate tetrahedral intermediates in the active center.

The notion that the hexamutant HuAChE or more significantly the multiple active center mutants are impaired in their capacity to stabilize tetrahedral species in the active center is consistent with the reactivity patterns of the HuAChE enzymes and of HuBChE toward methylphosphonates such as soman or IBMPF. Unlike the substrates and TMTFA, the free phosphate molecules have tetrahedral geometry, and it was suggested that their reactivity toward ChEs is determined to a large extent by the stability of the corresponding noncovalent phosphate−ChE Michaelis complexes (*22*, *54*, *55*). Accommodation of methylphosphonates by the HuAChE active center includes positioning of a methyl substituent in the acyl pocket in analogy to the acetyl methyl introduced in the tetrahedral intermediate of ATC or the trifluoromethyl substituent in the TMTFA−HuAChE adduct. The results demonstrate that the active center triple mutant HuAChE is impaired in reactivity toward soman and IBMPF to approximately the same extent as toward ATC or TMTFA (Table 3 and 4 and Figure 3). Thus, the diminished ability of the active center modified HuAChE to accommodate tetrahedral species, as compared to that of the wild-type HuAChE and that of HuBChE, is manifested for both covalently (tetrahedral intermediates of substrates and TMTFA) and noncovalently bound (Michaelis complexes with methyl phosphonates) species.

The analysis presented above, underscoring the HuBChE-like ability of the hexamutant HuAChE to accommodate ligands as long as they do not present a tetrahedral geometry like that of methylphosphonates, suggests the involvement of the catalytic His447. In the tetrahedral intermediate with substrate this residue is thought to interact with both the choline oxygen and the O_γ-Ser203 as a part of its function in catalysis of the hydrolytic reaction (*45*, *68*, *69*). In the X-ray structure of the TcAChE adduct with TMTFA, participation of the analogous residue His440 in accommodation of the tetrahedral adduct, is clearly visible (*66*). In various modeling experiments of AChE−phosphate Michaelis complexes, the catalytic histidine was also implicated in interaction with the oxygen of the P-alkoxy substituent (*21*, *22*, *27*). The precise juxtaposition of His447 was found to correlate with the facility of certain HuAChE−phosphonate conjugates to undergo a catalytic aging reaction (*45*, *69*). It appears from all these studies that minor changes in orientation of the His447 side chain, resulting from mutations at the HuAChE active center, may interfere therefore with accommodation of tetrahedral species. Examination of whether impaired accommodation of tetrahedral species in the butyryl-like mutants correlates with enhanced mobility of the His447 side chain was carried out by molecular simulation of residue motions at the active center (see Materials and Methods). The starting structure used in these experiments was taken from the X-ray structure of the HuAChE−fasciculin complex (*3*). Following initial equilibration at 3000 K, the main chain was constrained and motions of the side chains were examined at 4000 K. The results (see Figure 4) seem to suggest that while in the wild-type HuAChE the side chain of His447 maintains a similar average orientation as in the X-ray structure of HuAChE

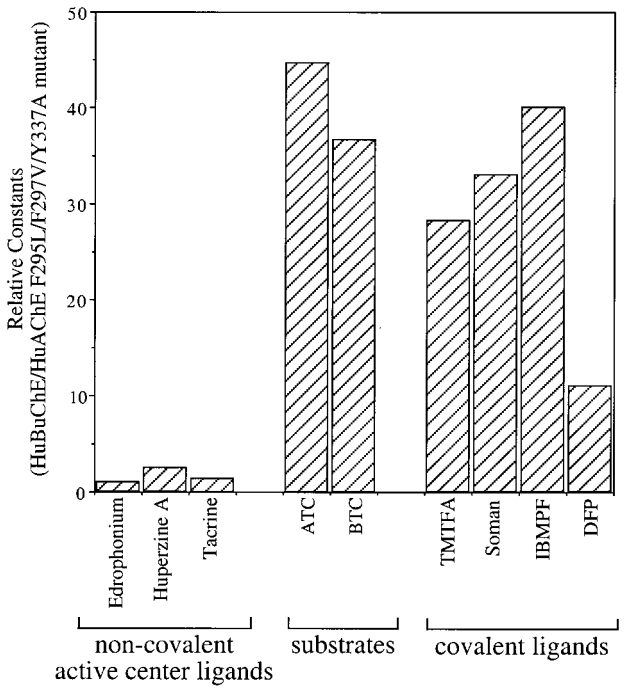

FIGURE 3: Relative reactivities of HuBChE and the triple active center mutant (F295L/F297V/Y337A) of HuAChE toward active center ligands. Shown are the relative values of the inhibition constants (K_i; see Table 5) for the noncovalent inhibitors edrophonium, huperzine A, and tacrine; of the apparent bimolecular rate constants for substrate hydrolysis of ATC and BTC (Table 1); and of the bimolecular rate constants of inhibition by the covalent ligands TMTFA, soman, IBMPF, and DFP (see Tables 3 and 4).

(Figure 4A), in the F295L/F297V/Y337A and in the hexamutant HuAChEs (Figure 4B,C) it tends to assume a different average conformation. This mobility results in breaking of the H-bond with the catalytic Ser203 (Figure 4B,C and Figure 5). This conformational transition of His447 seems to be irreversible within the time scale of our simulations. While one should be careful about attributing any specific role to the altered His447 conformation, the enhanced His447 mobility in the two mutant enzymes is consistent with their impaired ability to accommodate tetrahedral species. In fact, such mobility of the catalytic histidine, in apparent response to steric changes in the active center, has recently been observed in the X-ray structure of the TcAChE−VX conjugate (*70*). Steric changes due to multiple mutations at the HuAChE active center may also result in perturbation of its water structure (*6*). Specific water molecules in TcAChE and HuAChE were shown to play a major role in maintaining the orientation of His447 through the H-bond network (*3*, *22*, *49*).

If replacement of aromatic residues in the HuAChE active center produces a HuBChE-like architecture and at the same time alters the mobility of the catalytic histidine, the obvious question is why the same effect is not evident in HuBChE? It is reasonable to assume that in HuBChE an analogous perturbation to the positioning of the catalytic histidine is compensated by other interactions, yet an inquiry regarding the nature of these interaction as well as the residues participating in them is hardly possible without the X-ray structure of the enzyme. The results of the present study allude indeed to some differences in steric interactions within the active center, between the hexamutant HuAChE and

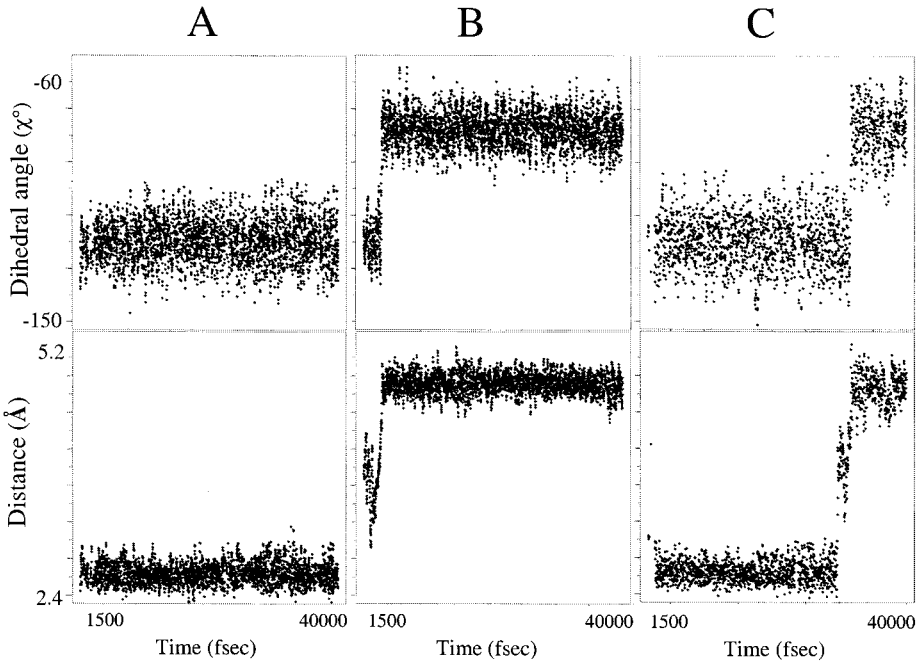

FIGURE 4: Examination of conformational mobility of the catalytic histidine side chain by molecular dynamics simulation. Depicted are 40 ps simulations performed on (A) wild-type HuAChE, (B) the triple active center mutant F295L/F297V/Y337A, and (C) the hexamutant Y72N/Y124Q/W286A/F295L/F297V/Y337A. Top panels: time dependence of the dihedral angle between the imidazolium moiety of His447 and the backbone ($\chi°$). Lower panels: time dependence of the distance between Nϵ_2-His447 and γ-Ser203 (Å). Extension of simulation time (up to 160 ps) did not result in any further changes of these conformational parameters.

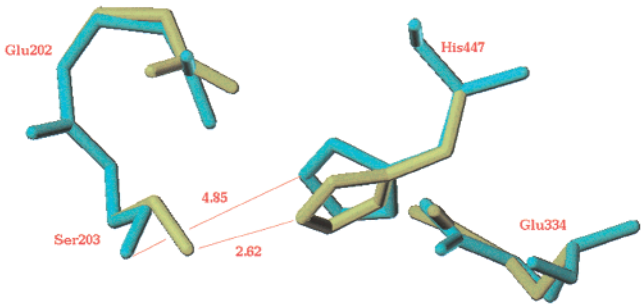

FIGURE 5: Potential modification of the optimal juxtaposition of the catalytic triad elements of the triple active center mutant and the hexamutant HuAChEs. The relative positions of Glu-His-Ser in the wild-type enzyme (yellow line) and in the mutant enzymes (blue line) are as suggested by molecular dynamics simulations (see Figure 4). Note that, in the mutants devoid of the three active center aromatic residues, disruption of the H-bond interaction between the catalytic His and Ser is a consequence of displacement of the side chains of both of these residues, resulting in an increase of the Nϵ_2-His447 and Oγ of Ser203 distance from 2.62 Å in WT to 4.85 Å.

HuBChE. These differences may be responsible for the small reactivity variations toward large ligands such as huperzine A or BW284C51 and for the dissociation rate constant (k_{off}) values of the corresponding TMTFA adducts. In addition, while multiple mutations at the HuAChE active center gorge abolish substrate inhibition, the HuBChE-like phenotype of substrate activation could not be achieved. Another finding that suggests a somewhat different array of steric interactions with catalytic histidine in HuBChE is the nearly equivalent reactivity of the hexamutant HuAChE and HuBChE with the organophosphate DFP. As with phosphonates these reactions involve initial noncovalent accommodation of the tetrahedral phosphate. Yet, in the case of DFP the substituent introduced into the acyl pocket is very large and may result in some distortion of the pocket in HuAChE. In fact, a recent X-ray structure of the TcAChE−DFP adduct shows that the isopropoxy substituent pointing toward the acyl pocket distorts the main chains of both the acyl pocket and part of the peripheral site (*56*). In the triple active center mutant HuAChE the accommodation of DFP seems to be impaired in a manner similar to that of other phosphate ligands, compared to HuBChE. Yet, during formation of the hexamutant HuAChE−DFP Michaelis complex, introduction of the bulky substituent into the void volume of the active center gorge may compensate for the aromatic replacements with respect to the proposed mobility of His447.

In summary, comparison of reactivity profiles of the Y72N/Y124Q/W286A/F295L/F297V/Y337A hexamutant HuAChE and of HuBChE suggests that the active center overall architecture, which is responsible for noncovalent accommodation of ligands, is not very sensitive to local perturbations resulting from mutagenesis. Therefore, the enzymatic characteristics of hexamutant HuAChE seem to be consistent with previous indications that AChE and BChE active centers differ predominantly in the volume of ligands they can accommodate. On the other hand, the precise juxtaposition of the catalytic residues (His and Ser) appears to be more sensitive to changes in the active center. Thus, the fact that the hexamutant HuAChE does not mimic the reactivity of HuBChE toward substrates and other covalent ligands may suggest that the catalytically productive orientation of the histidine in butyrylcholinesterase is maintained by a somewhat different array of interactions than that in acetylcholinesterase.

ACKNOWLEDGMENT

We thank Dr. Moshe Leitner for DNA synthesis, Mrs. Nechama Zeliger for excellent technical assistance, and Dr. Sara Cohen for critical reading of the manuscript.

REFERENCES

1. Sussman, J. L., Harel, M., Frolow, F., Oefner, C., Goldman, A., Toker, L., and Silman, I. (1991) *Science 253*, 872−879.
2. Bourne, Y., Taylor, P., and Marchot, P. (1995) *Cell 83*, 503−512.
3. Kryger, G., Harel, M., Giles, K., Toker, L., Velan, B., Lazar, A., Kronman, C., Barak, D., Ariel, N., Shafferman, A., Silman, I., and Sussman, J. L. (2000) *Acta Crystallogr. 56*, 1385−1394.
4. Harel, M., Kryger, G., Rosenberry, T. L., Mallender, W. D., Lewis, T., Fletcher, R. J., Guss, J. M., Silman, I., and Sussman, J. L. (2000) *Protein Sci. 9*, 1063−1072.
5. Axelsen, P. H., Harel, M., Silman, I., and Sussman, J. L. (1994) *Protein Sci. 3*, 188−197.
6. Koellner, G., Kryger, G., Millard, C. B., Silman, I., Sussman, J. L., and Steiner, T. (2000) *J. Mol. Biol. 296*, 713−735.
7. Botti, S. A., Felder, C., Lifson, S., Sussman, J. L., and Silman, I. (1999) *Biophys. J. 77*, 2430−2450.
8. Ordentlich, A., Barak, D., Kronman, C., Flashner, Y., Leitner, M., Segall, Y., Ariel, N., Cohen, S., Velan, B., and Shafferman, A. (1993) *J. Biol. Chem. 268*, 17083−17095.
9. Vellom, D. C., Radic, Z., Li, Y., Pickering, N. A., Camp, S., and Taylor, P. (1993) *Biochemistry 32*, 12−17.
10. Barak, D., Kronman, C., Ordentlich, A., Ariel, N., Bromberg, A., Marcus, D., Lazar, A., Velan, B., and Shafferman, A. (1994) *J. Biol. Chem. 269*, 6296−6305.
11. Taylor, P., and Radic, Z. (1994) *Annu. Rev. Pharmacol. Toxicol. 34*, 281−320.
12. Harel, M., Sussman, J. L., Krejci, E., Bon, S., Chanal, P., Massoulie, J., and Silman, I. (1992) *Proc. Natl. Acad. Sci. U.S.A. 89*, 10827−10831.
13. Cygler, M., Schrag, J. D., Susman, J. L., Harel, M., Silman, I., Gentry, M. K., and Doctor, B. P. (1993) *Protein Sci. 2*, 366−382.
14. Massoulie, J., Pezzementi, N., Bon, S., Krejci, E., and Vallette, F. M. (1993) *Prog. Neurobiol. 4*, 31−91.
15. Augustinsson, K. B. (1948) *Acta Physiol. Scand., Suppl. 52*, 1−182.
16. Shafferman, A., Velan, B., Ortentlich, A., Kronman, C., Grosfeld, H., Leitner, M., Flashner, Y., Cohen, S., Barak, D., and Ariel, N. (1992) *EMBO J. 11*, 3561−3568.
17. Radic, Z., Pickering, N. A., Vellom, D. C., Camp, C., and Taylor, P. (1993) *Biochemistry 32*, 12074−12084.
18. Jarv, J. (1984) *Bioorg. Chem. 12*, 259−278.
19. Benschop, H. P., and De Jong, L. P. A. (1988) *Acc. Chem. Res. 21*, 368−374.
20. Barak, D., Ariel, N., Velan, B., and Shafferman, A. (1992) in *Multidisciplinary Approaches to ChE Functions* (Shafferman, A., and Velan, B., Eds.) pp 177−183, Plenum Press, New York.
21. Hosea, N. A., Berman, H. A., and Taylor, P. (1995) *Biochemistry 34*, 11528−11536.
22. Ordentlich, A., Barak, D., Kronman, C., Ariel, N., Segall, Y., Velan, B., and Shafferman, A. (1996) *J. Biol. Chem. 271*, 11953−11962.
23. Ariel, N., Ordentlich, A., Barak, D., Bino, T., Velan, B., and Shafferman, A. (1998) *Biochem. J. 335*, 95−102.
24. Loewenstein-Lichtenstein, Y., Glick, D., Gluzman, N., Sternfeld, M., Zakut, H., and Soreq, H. (1996) *Mol. Pharmacol. 50*, 1423−1431.
25. Saxena, A., Redman, A. M., Jiang, X., Lockridge, O., and Doctor, B. P. (1997) *Biochemistry 36*, 14642−14651.
26. Gnatt, A., Loewenstein, Y., Yaron, A., Schwarz, M., and Soreq, H. (1994) *J. Neurochem. 62*, 749−755.
27. Ordentlich, A., Barak, D., Kronman, C., Benschop, H. P., De Jong, L. P. A., Ariel, N., Barak, R., Segall, Y., Velan, B., and Shafferman, A. (1999) *Biochemistry 38*, 3055−3066.
28. Radic, Z., Duran, R., Vellom, D. C., Li, Y., Cervenansky, C., and Taylor, P. (1994) *J. Biol. Chem. 269*, 11233−11239.
29. Schalk, I., Ehret-Sabatier, L., Le Feuvre, Y., Bon, S., Massoulie, J., and Goeldner, M. (1995) *Mol. Pharmacol. 48*, 1063−1067.
30. Nachon, F., Ehret-Sabatier, L., Loew, D., Colas, C., van Dorsselaer, A., and Goeldner, M. (1998) *Biochemistry 37*, 10507−10513.
31. Masson, P., Froment, M. T., Bartels, C. F., and Lockridge, O. (1996) *Eur. J. Biochem. 235*, 36−48.
32. Nachmansson, D., and Wilson, I. B. (1951) *Adv. Enzymol. 12*, 259−339.
33. Radic, Z., Reiner, E., and Taylor, P. (1991) *Mol. Pharmacol. 39*, 98−104.
34. Cauet, G., Friboulet, A., and Thomas, D. (1987) *Biochem. Cell Biol. 65*, 529−535.
35. Masson, P., Legrand, P., Bartels., C. F., Froment, M. T., Schopfer, L. M., and Lockridge, O. (1997) *Biochemistry 36*, 2266−2277.
36. Masson. P., Xie, W., Froment, M. T., Levitsky, V., Fortier, P. L., Albert, C., and Lockridge, O. (1999) *Biochim. Biophys. Acta 1433*, 281−293.
37. Soreq, H., Ben-Aziz, R., Prody, C. A., Seidman, S., Gnatt, A., Neville, L., Lieman-Hurwitz, J., Lev-Lehman, E., Ginzberg, D., Lipidot-Lifson, Y., and Zakut, H. (1990) *Proc. Natl. Acad. Sci. U.S.A. 87*, 9688−9692.
38. Velan, B., Grosfeld, H., Kronman, C., Leitner, M., Gozes, Y., Lazar, A., Flashner, Y., Marcus, D., Cohen, S., and Shafferman, A. (1991) *J. Biol. Chem. 266*, 23977−23984.
39. Kronman, C., Velan, B., Gozes, Y., Leitner, M., Flashner, Y., Lazar, A., Marcus, D., Sery, T., Papier, Y., Grosfeld, H., Cohen, S., and Shafferman, A. (1992) *Gene 121*, 295−304.
40. Shafferman, A., Kronman, C., Flashner, Y., Leitner, S., Grosfeld, H., Ordentlich, A., Gozes, Y., Cohen, S., Ariel, N., Barak, D., Harel, M., Silman, I., Sussman, J. L., and Velan, B. (1992) *J. Biol. Chem. 267*, 17640−17648.
41. Velan, B., Kronman, C., Ordentlich, A., Flashner, Y., Leitner, S., Cohen, S., and Shafferman, A. (1993) *Biochem. J. 296*, 649−656.
42. Prody, C. A., Zevin-Sonkin, D., Gnatt, A., Goldberg, O., and Soreq, H. (1987) *Proc. Natl. Acad. Sci. U.S.A. 84*, 3555−3559.
43. Arpagaus, M., Kott, M., Vatsis, K. P., Bartels, C. F., La Du, B. N., and Lockridge, O. (1990) *Biochemistry 29*, 124−131.
44. Nair, H. K., Lee, K.,and Quinn, D. M. (1993) *J. Am. Chem. Soc. 115*, 9939−9941.
45. Barak, D., Ordentlich, A., Segall, Y., Velan, B., Benschop, H. P., De Jong, L. P. A., and Shafferman, A. (1997) *J. Am. Chem. Soc. 119*, 3157−3158.
46. Benschop, H. P., Konings, C. A. G., Van Genderen, J., and De Jong, L. P. A (1984) *Toxicol. Appl. Pharmacol. 72*, 61−74.
47. Ellman, G. L., Courtney, K. D., Andres, V., and Featherstone, R. M. (1961) *Biochem. Pharmacol. 7*, 88−95.
48. Nair, H. K., Seravalli, J., Arbuckle, T., and Quinn, D. M. (1994) *Biochemistry 33*, 8566−8576.
49. Ordentlich, A., Kronman, C., Barak, D., Stein, D., Ariel, N., Marcus, D., Velan, B., and Shafferman, A. (1993) *FEBS Lett. 334*, 215−220.
50. Millard, C., and Broomfield, C. (1992) *Biochem. Biophys. Res. Commun. 189*, 1280−1286.
51. Loewenstein, Y., Gnatt, A., Neville, L. F., and Soreq, H. (1993) *J. Mol. Biol. 234*, 289−296.
52. Ordentlich, A., Barak, D., Kronman, C., Ariel, N., Segall, Y., Velan, B., and Shafferman, A. (1998) *J. Biol. Chem. 273*, 19509−19517.
53. Viragh, C., Harris, T. K., Reddy, P. M., Massiah, M. A., Mildvan, A. S., and Kovach, I. M. (2000) *Biochemistry 39*, 16200−16205.
54. Aldrich, W. N., and Reiner, E. (1972) in *Enzyme Inhibitors as Substrates* (Neuberger, A., and Tatum, E. L., Eds.) Elsevier, Amsterdam.
55. Main, A. R. (1976) in *Biology of Cholinergic Function* (Goldberg, A. M., and Hanin, I., Eds.) pp 269−353, Raven Press, New York.

56. Millard, C. B., Kryger, G., Ordentlich, A., Greenblatt, H., Harel, M., Raves, M., Segall, Y., Barak, D., Shafferman, A., Silman, I., and Sussman, J. L. (1999) *Biochemistry 38*, 7032−7039.
57. Ordentlich, A., Barak, D., Kronman, C., Ariel, N., Segall, Y., Velan, B., and Shafferman, A. (1995) *J. Biol. Chem. 270*, 2082−2091.
58. Ashani, Y., Grunwald, J., Kronman, C., Velan, B., and Shafferman, A. (1994) *Mol. Pharmacol. 45*, 555−560.
59. Saxena, A., Quian, N., Kovach, I. M., Kozikowski, A. P., Pang, Y. P., Vellom, D. C., Radic, Z., Quinn, D., Taylor, P., and Doctor, B. P. (1994) *Protein Sci. 3*, 1770−1778.
60. Silman, I., Harel, M., Axelsen, P., Raves, M., and Sussman, J. L. (1994) *Biochem. Soc. Trans. 22*, 745−749.
61. Harel, M., Schalk, I., Ehret-Sabatier, L., Bouet, F., Goeldner, M., Hirth, C., Axelsen P. H., Silman, I., and Sussman, J. L. (1993) *Proc. Natl. Acad. Sci. U.S.A. 90*, 9031−9035.
62. Bourne, Y., Grassi, J., Bougis, P. E., and Marchot, P. (1999) *J. Biol. Chem. 274*, 30370−30376.
63. Chatonnet, A., and Lockridge, O. (1989) *Biochem. J. 260*, 625−634.
64. Soreq, H., and Zakut, H. (1990) *Prog. Brain Res. 84*, 51−61.
65. Doctor, B. P., Chapman, T. C., Christner, C. E., Deal, C. D., De La Hoz, D. M., Gentry, M. K., Ogert, R. A., Rush, R. S., Smyth, K. K., and Wolfe, A. D. (1990) *FEBS Lett. 266*, 123−127.
66. Harel, M., Quinn, D. M., Nair, H. K., Silman, I., and Sussman, J. L. (1996) *J. Am. Chem. Soc. 118*, 2340−2346.
67. Radic, Z., Kirchhoff, P. D., Quinn, D. M., McCammon, J. A., and Taylor, P. (1997) *J. Biol. Chem. 272*, 23265−23277.
68. Bencsura, A., Enyedy, I., and Kovach, I. M. (1995) *Biochemistry 34*, 8989−8999.
69. Shafferman, A., Ordentlich, A., Barak, D., Stein, D., Ariel, N., and Velan, B. (1996) *Biochem. J. 32*, 996−998.
70. Millard, C. B., Koellner, G., Ordentlich, A., Shafferman, A., Silman, I., and Sussman, J. L. (1999) *J. Am. Chem. Soc. 121*, 9883−9884.
71. Massoulie, J., Sussman, J. L., Doctor, B. P., Soreq, H., Velan, B., Cygler, M., Rotundo, R., Shafferman, A., Silman, I., and Taylor, P. (1992) in *Multidisciplinary Approaches to Cholinesterase Functions* (Shafferman, A., and Velan, B., Eds.) pp 285−288, Plenum Press, New York.

BI010181X